Dissipative Frenkel-Kontorova chains

Wolfgang Quapp[1*] and Josep Maria Bofill[2,3]

[1*]Mathematisches Institut, Universität Leipzig, D-04009 Leipzig, PF 100920, Germany.

[2]Departament de Química Inorgànica i Orgànica, Secció de Química Orgànica, Universitat de Barcelona, Martí i Franquès 1, Barcelona, 08028, Spain.

[3]Institut de Química Teòrica i Computacional, (IQTCUB), Universitat de Barcelona, Martí i Franquès 1, Barcelona, 08028, Spain.

*Corresponding author(s). E-mail(s): quapp@math.uni-leipzig.de;
Contributing authors: jmbofill@ub.edu;

Abstract

We rebut the use of a questionable method, DSM iteration (dissipative standard map), for calculating a finite dissipative Frenkel-Kontorova chain. It should be replaced by a standard optimization method, connected for instance by the Newton trajectory method.

Keywords: dissipative Frenkel Kontorova chain, Newton trajectory, dissipative standard map

. Received: March 14, 2026

1 Introduction: the FK model

In recent contributions to Physica D [1, 2] Afsar and co-workers reported on computational studies of dissipative Frenkel-Kontorova (FK) chains. Dissipative here means that the bonds between all atoms in the chain are different. Our criticism is directed against the use of a method for calculating the energy of an FK atomic chain with atoms at positions x_i on the x-axis with $x_i < x_{i+1}$, as well as of the formula of the

energy itself

$$H = \sum_{n=1}^{N} (1-\gamma)^{-n} \left[(x_n - x_{n-1} - \Omega)^2 - \frac{K}{(2\pi)^2} cos(2\pi x_n) \right] . \tag{1}$$

The *cosinus* function represents a substrate potential in which the chain is embedded. Often one depicts H the potential energy hypersurface (PES), $H(\mathbf{x})$. The dissipation is caused by the γ-factors with $\gamma \in (0, 1)$. However, the given ansatz (1) appears questionable, as it extends dissipation to the side potential as well. This, in contrast, should be independent on the random filling with an arbitrary x_n. The side potential should be a normal periodic potential, as shown in Fig. 1 of ref. [2]. We propose to use

$$H = \sum_{n=1}^{N} \left[(1-\gamma)^{-n} (x_n - x_{n-1} - \Omega)^2 - \frac{K}{(2\pi)^2} cos(2\pi x_n) \right] \tag{2}$$

where a pair of brackets is shifted. Eq.(2) in [1] begins with x_0 in the sum, so that the chain has $(N+1)$ atoms, not N. (But x_0 can be fixed, it is not directly subject of optimization.) For x_0 there is no substrate potential in Eq.(1) in [1]. We have freely set it to zero energy at coordinate $x_0 = 0.1$ (as in other cases, see below).

The gradient system of Eq.(2) has a slightly different form than in [1]

$$\begin{aligned} 0 = \frac{\partial H}{\partial x_n} &= -(x_{n+1} - x_n) + (1-\gamma)(x_n - x_{n-1}) + \\ &\gamma\,\Omega + \frac{(1-\gamma)^{n+1} K}{4\pi} sin(2\pi x_n), \;\; n = 1, .., N-1 \; . \end{aligned} \tag{3}$$

A factor of $\frac{(1-\gamma)^{n+1}}{2}$ must be used at the *sin* term for our ansatz (2); in the original formula (1), the larger factor of $\frac{(1-\gamma)}{2}$ would be missing. The missing factor is (in every case) already incorrect in refs. [2, 3]. Therefor, the FK model is not suitable for a DSM ansatz. Work [4] discusses a DSM formula for an FK chain, but the authors do not provide an explicit formula for the FK energy. So, we cannot accept their approach. We believe that the original intention of the DSM in refs. [3, 5–9] is not fulfilled by either of the two energy formulas. Note that the original development of the DSM was to model a kicked rotator [7, 10] or a charged particle in the electric field of a electromagnetic wave packet [8]. These were not FK models.

In case (1), one could apply a factor $\tilde{K} = (1-\gamma)\,K$ with an adapted constant for K. Thus, the iterations of DSM could be corrected, however, a deeper error is that system (3) in [1] does not take into account the last equation for atom x_N. This additional last line for the system (3) for x_N is

$$0 = \frac{\partial H}{\partial x_N} = x_N - x_{N-1} - \Omega + \frac{(1-\gamma)^N K}{4\pi} sin(2\pi x_N) \; . \tag{4}$$

However, the $(N-1)$th equation in (3) is

$$0 = \frac{\partial H}{\partial x_{N-1}} = -(x_N - x_{N-1}) + (1-\gamma)\,(x_{N-1} - x_{N-2}) + \gamma\,\Omega + \frac{(1-\gamma)^N\,K}{4\pi} sin(2\pi x_{N-1}) \tag{5}$$

and this contradicts Eq. (4) for the variable x_N in the general case. Consequences are explained in Section 2 below.

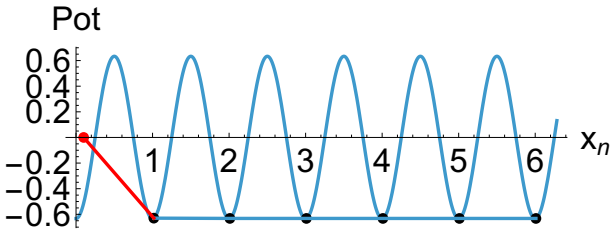

Fig. 1 Global minimum of the FK model of Afsar et al., modified to formula (2). Pot is the energy of the side potential. The red boundary point is set to $x_0 = 0.1$. Other atoms are optimized. For better visibility, the atoms are shifted on the substrate potential. The varying strengths of the bonds between the atoms are slightly indicated by the increasing thickness.

The authors of ref. [1] fix x_1, whereas we fix x_0; this is an equivalent action. (For a fixed x_1, the first equation in system (3) would be useless, but then would be x_0 open, and we had an $(N-1)$-dimensional gradient system but with an analogous property.) Note that we do not have a free-end chain as it is claimed in the abstract and in line 1 of section 2 in [1]. This point is important; it is another model. Using models (1) or (2) and excluding a fixed atom x_0, the chain with a free x_1 will have another minimum structure, in comparison with the chain with x_1 connected to a fixed x_0.

For a finite N, an optimization calculation can be performed for the structure of an equilibrium chain, see Fig. 1. We use $K = 25, \gamma = 0.9, \Omega = 1$, and $N = 6$, atom x_0 is fixed and x_1 can move. A corresponding minimum is at
x=(0.1, 1.02, 2.01, 3.01, 4.01, 5.01, 6.01) with H=-3.65.

It is obvious that the model of strong strings in Eq.(2) forces a chain close to the lowest points of the side potential with distances $x_n - x_{n-1} \approx \Omega$. This also occurs for some further possible minima and a saddle point (SP) in Fig. 2. The different minimum structures are moved on the axis; they arise by shifting x_0 on the interval (0,1) as in [1], but above all, by different start chains for the optimization. We have found the chains:
a) **x**=(0.05, 0.19, 1.12, 2.12, 3.12, 4.12, 5.12), H=5.31
b) **x**=(0.31, 1.07, 2.05, 3.05, 4.05, 5.05, 6.05), H=-1.54
c) **x**=(0.61, 1.91, 2.94, 3.94, 4.94, 5.94, 6.94), H=-1.11
d) **x**=(0.05, 1.83, 2.89, 3.9, 4.9, 5.9, 6.9), H=3.67
State (a) is an anti-kink, whereas state (d) is a kink. Both states have more energy.

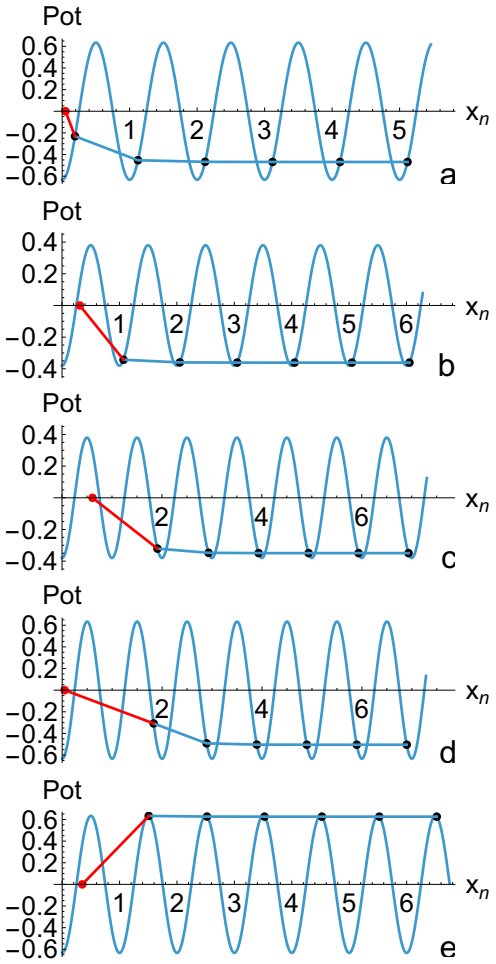

Fig. 2 FK minima as in Fig. 1 for (a) $K = 25$ and $x_0 = 0.05$. We start with a movement of the chain to the left hand side, and indeed there is such a minimum. For the weakest bond between x_0 and x_1, the distance is reduced. (b) $K = 15$ and $x_0 = 0.31$: The chain has a little moved but the atoms still are in their bowls. (c) $K = 15$ and $x_0 = 0.61$, we start with a movement to the right hand side, and there is a minimum where the chain is moved one bowl further. (d) $K = 25$ and $x_0 = 0.05$, we start with a movement to the right, and there is a chain in a labile equilibrium structure, a shoulder point with a zero eigenvalue of the Hessian matrix. (e) is an SP of index 1.

However, these states cannot move like a soliton [11, 12], due to the dissipative nature of the potential (2).

Various stationary chains in Fig. 2 show that there is more than one minimum structure. There is also a dependency on K. For low K values, the strong strings in Eqs.(1) or (2) lead to a simple chain with $x_n \approx n$. There is also a transition state, a normal SP of index one, at

e) $\mathbf{x}$=(0.35, 1.51, 2.52, 3.52, 4.52, 5.52, 6.52), H=4.04,

where all atoms x_n are more or less at the peak of the side potential, again with

distances between the atoms at $\approx \Omega$. This transition state depicts the step from a chain of type (a) to a chain of type (c) or (d).

In general, stationary structures can be found using the method of Newton trajectories [13–15], see section 3.

2 The DSM iteration works not correct – an intrinsic comment

If one fix $p_1 = x_1 - x_0$ (a logical continuation of the p_n-definition downwards in [1]), this determines x_2 in the first equation of system (3), then x_3 in the next, and so on, i.e. the entire DSM iteration of [1]. However, the system of N equations cannot be solved by a prescription of one variable. Because the last equation (4) is usually not satisfied.

Of course, if one starts with the 'correct' x_0, x_1 of a minimal chain, i.e. a correctly fixed p_1, the DSM iteration works correctly. But note that any tiny numerical deviation of an atom x_n (by an approximation of π or the *sinus*-function) causes the entire end of the chain to deviate. As N increases, such numeric errors can accumulate.

However, starting with random boundary values will fail. In the FK chain, one can it imagine by the back action of the last atoms on the atom x_1. This means that the claim that (x_1, p_1) can be chosen at random is incorrect. Most of the calculations of paper [1] are false, if they are understood as values for an FK chain in equilibrium with a fixed x_0. If an iteration starts incorrectly, all other values are also false.

And if N becomes larger in ref. [1] then the exorbitant deep harmonic potentials in (1) or (2) for $\gamma = 0.9$ also enforce a distance that is quasi equal to Ω between every pair x_n and x_{n+1} for larger values of n. Thus, different equilibrium structures of the chain seem to be possible only for different movements of the first atoms of the chain, as it is the case in Fig. 2.

We firmly refuse the results regarding the bifurcations of (FK minimum structure)-energies. They are connected with the (incorrectly) used dissipative standard map iterations with incorrect starting points. We point out that we already discussed the corresponding problems several years ago [15–19]. The point is the fundamental failure of the so-called Aubry theory. Works that use this theory, see [3, 20, 21] to name but a few, shift the boundaries of the chain to $\pm\infty$. However, this is not manageable for computational studies. Therefor, like the works [1, 2], they start at arbitrary points on the iteration ladder, thus with arbitrary start points. Here, too, we must conclude that this way is incorrect: Ex falso quodlibet.

From the point of view of Mathematics, we could not find any proof of convergence in the corresponding papers. This would be necessary for handling with infinity.

A scurrile way to verify some of the calculations of Refs. [1, 2] for a finite N could be to compare the final values of x_N of the two Eqs.(4) and (5). If these are equal, the entire chain is a correct stationary state. We guess that very few structures in [1] meet this condition.

3 Application of Newton trajectories (NT)

An NT is a curve in which, at every point, the gradient of the PES points in the same normalised direction $\mathbf{f}$

$$\mathbf{g}(\mathbf{x}) = F\,\mathbf{f}\,, \tag{6}$$

where $\mathbf{g}$ is the gradient of the PES. The value F is the norm of the gradient. It changes as a non-linear parameter along the solution.

There is a differential equation along the curve [22]

$$\frac{d\mathbf{x}}{dt} = Det(\mathbf{H})\mathbf{H}^{-1}(\mathbf{x})\,\mathbf{g}(\mathbf{x})\ . \tag{7}$$

$\mathbf{H}^{-1}$ is the inverse of the Hessian matrix of the PES, and $Det(\mathbf{H})$ is its determinant, and t is the curve length parameter. Solutions to Eqs. (6) and (7) are denoted as NT. Eq. (7) was formulated by Branin [23]. General solutions of Eqs. (6) and (7) in different directions $\mathbf{f}$ connect a minimum with a saddle point (SP) of index one, or they connect higher index SPs of an index difference of one. In this case of a dissipative FK model, the Hessian matrix quickly assumes very large entries as N increases. This makes the calculation somewhat complicated.

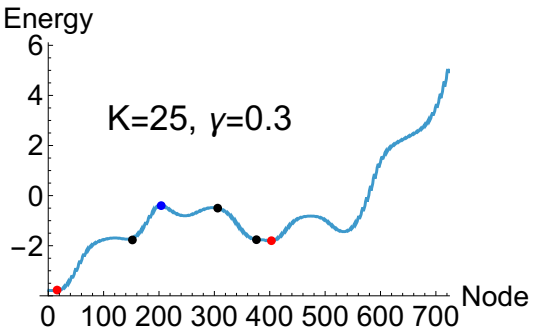

Fig. 3 Example of an energy profile over an NT for an FK calculation where H of Eq.(2) is the energy. Node counts the number of base points of the calculation. Start is at the global minimum. Red dots are minima, black points are SP_1 and blue is an SP_3. Further seemingly stationary points are turning points of the NT in the PES mountains.

3.1 Example

We try $\gamma = 0.3$ and form a model close to a typical FK chain, which is mild compared to the strong harmonic forces between the atoms in the dissipative model [1]. We use for the search direction the vector

$F\,\mathbf{f} = (-0.3, -0.15, -0.05, 0.2, 0.1, 0)$

where we 'pull' three atoms to the left side, and 'push' atoms 4 and 5 to the right side. For the usual constants $K = 25$ and $\Omega = 1$, we obtain an energy profile in Fig. 3. We can identify many stationary structures along the NT, see Fig.4.

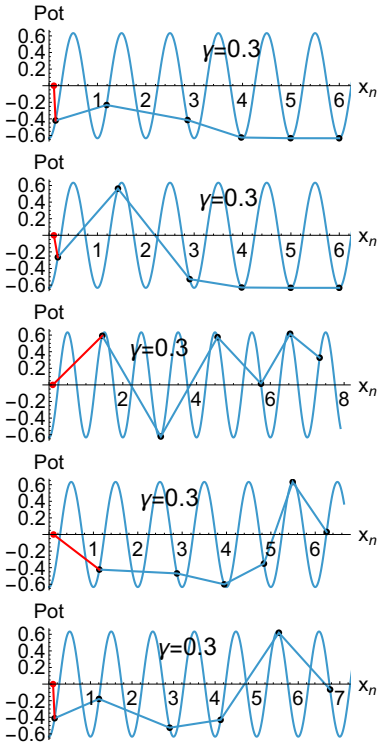

Fig. 4 FK structures to model (2) with $K = 25$ and $\gamma = 0.3$. Line 1 is a minimum with an anti-kink at 0 and a kink at position 2, which lies to the left of the global minimum. Along the profile in Fig. 3, starting from second line: SP_1 with an anti-kink at 0 and a kink at 1 and 2; an SP_3 with three atoms on the tips of the side potential; two further SP_1 with first a kink at position 2 and an anti-kink at 5 and 6; and the second has an anti-kink at 0 and a kink at 5 and 6.

It is obvious that the slight change in the usual FK model by $\gamma = 0.3$ allows us to explore the PES over wide ranges. However, the known solitones of the case $\gamma = 0$ do not occur here. And it is obvious that the NT of Fig. 4 forms loops.

The favourable possibilities for exploring the PES change with a higher value for γ. We try to explain this circumstances with some PES contour line pictures for different γ values. We start with $\gamma = 0$ in Fig. 5 where x_1 and x_2 are symmetric for their harmonic potentials. In order to draw a two-dimensional figure, we project out the remaining atoms. We only need to consider the distance to atom x_3. We use the plane $x_3 = 0.5\,(3 + x_1 + x_2)$. It is clear that there are many paths for internal movements of the atoms within the chain.

Next we study the case $\gamma = 0.3$ in Fig. 6.

The case of $\gamma = 0.6$ in Fig. 7 becomes even stranger. We draw a projection of the contour lines in a skew plane $x_3 = 0.5\,(3 + x_1 + x_2)$. With this view we can observe three minima and two saddles in between. The blue line is an NT which connects all stationary points. (The NT is calculated in the complete 6-dimensional space; here is only shown the 2-dimensional part.) We draw the profile over the NT in Fig. 8. One may observe that such a calculation is already difficult: the steep slopes in Fig. 7, at the

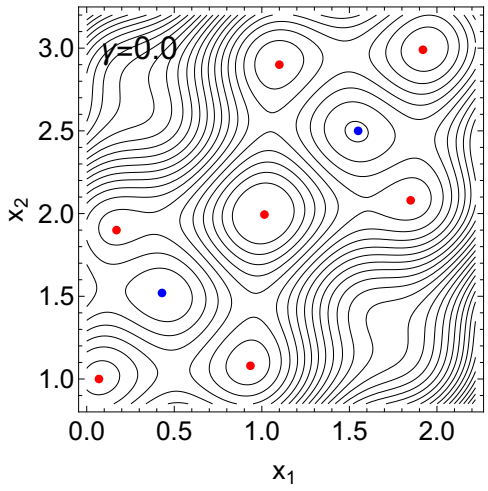

Fig. 5 Level lines of the PES for $K = 25$, $\gamma = 0$, and projection in the plane $x_3 = 0.5\,(3 + x_1 + x_2)$. Red points are minima, SPs of index 2 are blue.

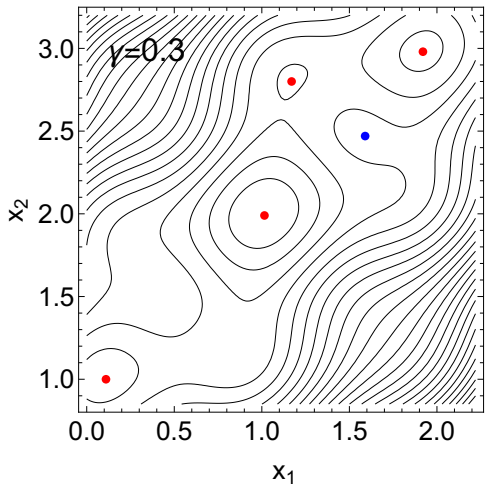

Fig. 6 PES for $K = 25$, $\gamma = 0.3$, projection in the plane $x_3 = 0.5\,(3 + x_1 + x_2)$. Red dots mark minima, one SP of index 2 has disappeared, as well as many minima of Fig. 5.

'corners' at the top left and bottom right, indicate that only NTs with a small range of search directions can be calculated well. This direction is determined heuristically, by trial and error. The NT is found with the search vector $F\,\mathbf{f} = (0.2, 0.3, 0.4, 0.45, 0.5, 0.5)$ which is a movement of all atoms in one direction. We had to use a very small step size for the calculation, and the convergence is poor. The occurrence of turning points (shown in green in Fig. 8) indicates the increasing difficulty with rising γ. We tried other search directions, but we could not find any with an NT without TPs. The stationary points (apart from the trivial minimum) of Fig. 8 are depicted in Fig. 9. The problems arise here because the bond between x_2 and x_3 becomes much stronger in

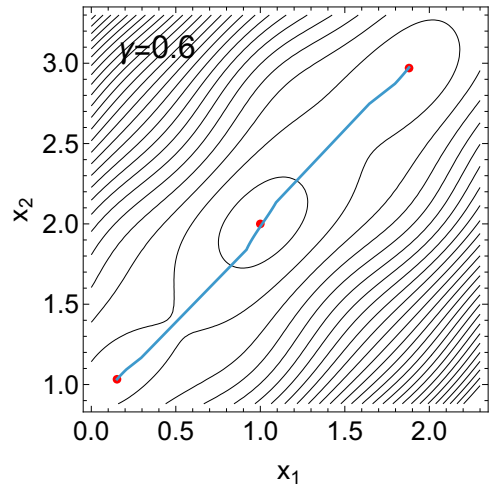

Fig. 7 PES for $K = 25$, $\gamma = 0.6$. We use a skew plane of x_3 for the projection. The blue line is the projection of an NT, see text. Red dots are minima. The central minimum is the global minimum at $(x_1, x_2, x_3) \approx (1, 2, 3)$. The SPs of index 2 from Fig. 5 have disappeared, as have many other minima.

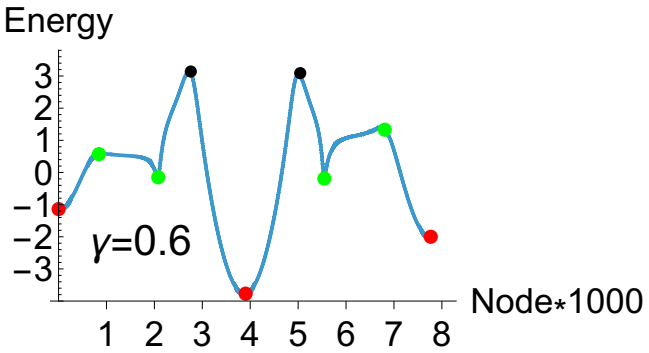

Fig. 8 Energy profile over an NT for $\gamma = 0.6$. Start is at the left minimum in Fig. 7. Red dots are minima, black dots are SP_1. Further seemingly stationary points in green are turning points of the NT on the slope of the PES.

this dissipative model. For $\gamma = 0.6$ we have strength factors for the first bond 2.5, for the second 2.5^2, but for the third by 2.5^3, and so on, up to 2.5^6. The chain becomes very stiff, compare Fig. 9. The development from $\gamma = 0$ to $\gamma = 0.3$ to $\gamma = 0.6$ shows the increasing stiffness of the corresponding chains. The larger γ becomes, the stiffer the chain of the right 'end'-atoms becomes. Only atoms x_1 and x_2 can form compressed or stretched structures. This is even more extreme in the structures of Fig. 2 for $\gamma = 0.9$. It is also demonstrated in Fig. 10 where only one minimum remains in the main valley. From this projection one would not expect the other stationary states of Fig. 2.

Here we can argue for our choice of only $N = 6$: examining longer chains up to $N = 100$, as in Refs. [1, 2] does not change the situation. The long 'right' end of the chain appears fixed.

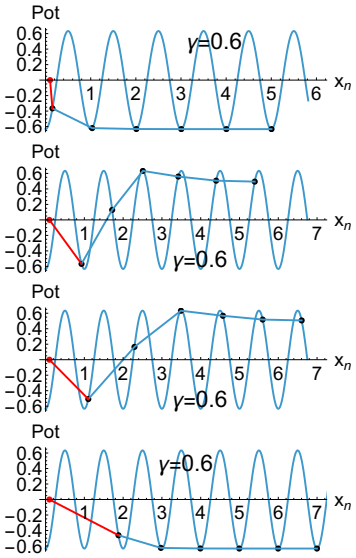

Fig. 9 FK structures to model (2) with $K = 25$ and $\gamma = 0.6$. First two lines are a left anti-kink minimum, and a subsequent SP_1, which can be seen in Fig. 7. The global minimum is omitted. Along the profile of Fig. 8 we then have an SP_1 and a kink of atom 2 at places 2 and 3; and the last is a minimum with a kink of atom 1 at place 2.

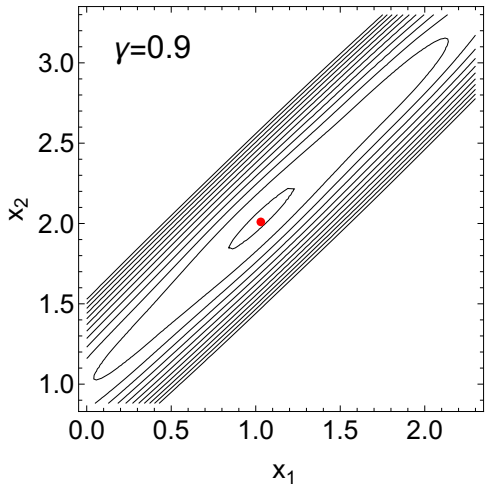

Fig. 10 PES for $K = 25$, $\gamma = 0.9$, projection onto the plane $x_3 = 0.5\,(3 + x_1 + x_2)$. In this plane, only one red dot marks a remaining minimum.

4 Conclusion

The papers [1, 2] do not correctly describe a Frenkel-Kontorova model, as the titles claim. In the general case, one cannot use the dissipative standard map with random start to find stationary structures of a finite FK chain and their energies. The DSM

iteration itself may be correctly reproduced with its bifurcations, but its fundament is open.

Dissipative FK chains are physically 'boring' for large $\gamma > 1/2$: they can only have different stationary structures at the left end of the chain. Note that there is also another definition of a dissipative force for FK chains [20, 21] which we do not discuss here.

Authorship contribution statement
Both authors contributed equally.

Data availability
The data will be made available upon request, as will the Mathematica procedures for minimising and for representation of the figures, and a Fortran program for calculating the NTs.

Conflict of Interest
There is no conflict of competing interests.

Acknowledgements
We acknowledge the financial support from the Spanish Structures of Excellence Mariá de Maeztu program, grant CEX2021-001202-M.

References

[1] Afsar, O., Saltik, S., Bughluyeva, F.: Exploring complexity of a Frenkel-Kontorova-type atomic chain. Physica D **486**, 135072 (2026)

[2] Afsar, O., Tirnakli, U.: Energy distribution of Frenkel-Kontorova-type atomic chains: Transition from conservative to dissipative dynamics. Physica D **470**, 134375 (2024)

[3] Wenzel, W., Biham, O., Jayaprakash, C.: Periodic orbits in the dissipative standard map. Phys. Rev. A **43**(12), 6550–6557 (1991)

[4] Ciubotariu, C., Bădeliţă, L., Stancu, V.: Chaos in dissipative relativistic standard maps. Chaos Solitons & Fractals **13**, 1253–1267 (2002) https://doi.org/10.1016/S0960-0779(01)00122-9

[5] Schmidt, G., Wang, B.W.: Dissipative standard map. Phys. Rev. A **32**(5), 2994–2999 (1985)

[6] Celletti, A., Di Ruzza, S.: Periodic and quasi-periodic orbits of the dissipative standard map. Disc. Cont. Dyn. Sys. B **16**(1), 151–171 (2011)

[7] Zhang, Y.P., Qiao, W., Sun, J.: Control and synchronization of Julia sets of complex standard family. Indian J. Phys. **87**(3), 271–274 (2013) https://doi.org/

10.1007/s12648-012-0220-1

[8] Horstmann, A.C.C., Albuquerque, H.A., Manchein, C.: The effect of temperature on generic stable periodic structures in the parameter space of dissipative relativistic standard map. Eur. Phys. J. B **90**, 96 (2017) https://doi.org/10.1140/epjb/e2017-70529-6

[9] Bustamante, A.P., Celletti, A., Lhotka, C.: Breakdown of rotational tori in 2D and 4D conservative and dissipative standard maps. Physica D **453**, 133790 (2023)

[10] Carlo, G.G., Ermann, L., Rivas, A.M.F., Spina, M.E., Poletti, D.: Classical counterparts of quantum attractors in generic dissipative systems. Phys. Rev. E **95**, 062202 (2017) https://doi.org/10.1103/PhysRevE.95.062202

[11] Joos, B.: Properties of solitons in the Frenkel-Kontorova model. Solid State Comm. **42**, 709–713 (1982)

[12] Quapp, W., Lin, J.Y., Bofill, J.M.: The movement of a one-dimensional Wigner solid explained by a modified Frenkel-Kontorova model. Eur. Phys. J. B **93**, 227 (2020)

[13] Quapp, W., Hirsch, M., Imig, O., Heidrich, D.: Searching for saddle points of potential energy surfaces by following a reduced gradient. J. Comput. Chem. **19**, 1087–1100 (1998)

[14] Anglada, J.M., Besalú, E., Bofill, J.M., Crehuet, R.: On the quadratic reaction path evaluated in a reduced potential energy surface model and the problem to locate transition states. J. Comput. Chem. **22**, 387–406 (2001)

[15] Quapp, W., Bofill, J.M.: Newton trajectories for the tilted Frenkel-Kontorova model. Molec. Phys. **117**, 1541–1558 (2019)

[16] Quapp, W., Bofill, J.M.: Comment on "out-of-equilibrium Frenkel-Kontorova model" by A.Imparato, 2021, J.Statit.Mech. 013214. J. Statist. Mech. **2022**, 013204 (2022)

[17] Quapp, W., Bofill, J.M.: An analysis of some properties and of the use of the twist map for the finite Frenkel-Kontorova model. Electronics **22**, 3295 (2022)

[18] Quapp, W., Bofill, J.M.: Letter: On putative incommensurate states of a finite Frenkel-Kontorova chain. arXiv2210.070000 (2022)

[19] Quapp, W., Bofill, J.M.: Das Frenkel-Kontorova Modell - eine unendliche Geschichte -. Leibniz Online **49**, 1–19 (2023)

[20] Floria, L.M., Mazo, J.J.: Dissipative dynamics of the Frenkel-Kontorova model. Adv. Phys. **45**, 505–598 (1996)

[21] Slijepčević, S.: Stability of syncronisation in dissipatively driven Frenkel-Kontorova model. Chaos **25**, 083108 (2015)

[22] Quapp, W., Bofill, J.M.: Reaction rates in a theory of mechanochemical pathways. J. Comput. Chem. **37**, 2467–2478 (2016)

[23] Branin, F.H.: Widely convergent methods for finding multiple solutions of simultaneous nonlinear equations. IBM J. Res. Develop. **16**, 504–522 (1972)